Learning of dynamics using basis elements

The internal model of the environmental torque is:

$$\hat{\tau}_{env} = \sum_i w_i \cdot g_i(\underline{z})$$

$\hat{\tau}_{env}$: the expected environmental torque.

$\underline{z}$: a desired state of the limb (consisting of limb position and velocity calculated with minimum jerk model).

g_i : a basis element.

w_i : a torque vector composed of shoulder torque and elbow torque, corresponding to each basis element.

In training, adaptation is realized by a trial-to-trial update of torque vectors following gradient descent:

$$\Delta w_i = \eta \cdot g_i(\underline{z}) \cdot \tilde{\tau}_{env} \ ,$$

$$\tilde{\tau}_{env} = \hat{\tau}_{env} - \tau_{env}$$

$\tilde{\tau}_{env}$: the difference between the actual torque experienced during the movement and the expectation of torque currently predicted by the internal model.

τ_{env} : the actual torque experienced during the movement.

η : learning rate

The basis elements represent the arm's position and velocity as a gain-field:

$$g(\underline{q}_d, \underline{\dot{q}}_d) = g_{position,i}(\underline{q}_d) \cdot g_{velocity,i}(\underline{\dot{q}}_d)$$

$$g_{position,i}(\underline{q}_d) = k_i^{\ T} \cdot \underline{q}_d + b$$

$$g_{velocity,i}(\underline{\dot{q}}_d) = \exp\left(\left\| \underline{\dot{q}}_d - \underline{\dot{q}}_i \right\|^2 / 2\sigma^2 \right)$$

$\underline{q}_d$ **:** a desired joint position, 2×1 vector composed of shoulder and elbow joint displacement.

$\underline{\dot{q}}_d$ **:** a desired joint velocity, 2×1 vector composed of shoulder and elbow joint velocity.

$\underline{\dot{q}}_i$: the preferred velocity .

k_i : a 2×1 vector composed of gradients for shoulder and elbow joint displacement. k_i can be decomposed into two components: magnitude and directional unit vector as

$$k_i = |k| \cdot \begin{bmatrix} \cos\theta_i \\ \sin\theta_i \end{bmatrix}.$$

b: intercept (constant) of a linear function.

σ : width of Gaussian function

All the parameters were fixed in the following manner: 1) The direction of positional gradients (θ_i) were uniformly distributed from 0° to 315° with a 45° increment. 2) The preferred velocities ($\underline{\dot{q}_i}$) are uniformly tiled in 2D joint velocity space with a 20.6 °/sec spacing and width (σ). The range of preferred joint velocity is [-103 °/sec, 103 °/sec] and [-165 °/sec, 165 °/sec] in shoulder and elbow axis respectively. 3) The total number of basis elements was equal to the number of the preferred positional gradients multiplied by the number of preferred velocities because we used every possible combination of gradient and preferred velocity. Thus, the total number of bases was 1496 (8 positional gradients ×187 preferred velocities). 4) The initial weight is zero. 5) The learning rate, η is 0.00014. 6) Random noise was injected into the torque in the simulated system so that movements in the null field had the same standard deviation of *p.e.* as the subjects' movements. The random noise used in our simulation was Gaussian noise with zero mean and 0.3 N·m standard deviation. 7) In exploring the parameter space of |*k*| and *b*, we found that a slope of 1 rad^{-1} and 1.3 intercept gave a good fit of interference as a function of separation distance.

Simulation of human arm reaching in 2D space

To simulate human arm reaching, we used the following model of the arm's dynamics that described the physics of our experimental setup (Shadmehr and Mussa-Ivaldi, 1994).

For every time step (10 ms), we calculate the joint acceleration ($\underline{\ddot{q}}$) using

$$\underline{\ddot{q}} = H(\underline{q})^{-1}\{H(\underline{q}_d)\underline{\ddot{q}}_d + C(\underline{q}_d, \underline{\dot{q}}_d)\underline{\dot{q}}_d - K_p(\underline{q} - \underline{q}_d) - K_v(\underline{\dot{q}} - \underline{\dot{q}}_d) - \hat{\tau}_{env} + \tau_{env} - C(\underline{q}, \underline{\dot{q}})\underline{\dot{q}}\}$$

where

$\underline{q}$: a 2×1 vector composed of shoulder and elbow joint displacement.

$\underline{\dot{q}}$: a 2×1 vector composed of shoulder and elbow joint velocity.

H: inertia matrix that varies as a function of joint displacement.

$$H(\underline{q}) = \begin{bmatrix} a_3 + a_1 \cdot l_1^{\,2} + a_4 + 2 \cdot a_2 \cdot l_1 \cdot \cos(q_{elbow}) & a_2 \cdot l_1 \cdot \cos(q_{elbow}) + a_4 \\ a_2 \cdot l_1 \cdot \cos(q_{elbow}) + a_4 & a_4 \end{bmatrix}$$

C: coriolis matrix that varies as function of joint displacement and velocity.

$$C(\underline{q}, \dot{\underline{q}}) = \begin{bmatrix} -a_2 \cdot l_1 \cdot \sin(q_{elbow}) \cdot \dot{q}_{elbow} & -a_2 \cdot l_1 \cdot \sin(q_{elbow}) \cdot (\dot{q}_{shoulder} + \dot{q}_{elbow}) \\ a_2 \cdot l_1 \cdot \sin(q_{elbow}) \cdot \dot{q}_{shoulder} & 0 \end{bmatrix}$$

K_p, K_v : spinal and muscle feedback coefficient.

τ_{env} : the actual torque experienced during the movement, followed the rule

$\tau_{env} = J^T \cdot F_{env} = J^T \cdot B \cdot \dot{\underline{x}}$

J : jacobian matrix that varies as a function of arm position

$$J = \begin{bmatrix} -l_1 \cdot \sin(q_{shoulder}) - l_2 \cdot \sin(q_{shoulder} + q_{elbow}) & l_2 \cdot \sin(q_{shoulder} + q_{elbow}) \\ l_1 \cdot \cos(q_{shoulder}) + l_2 \cdot \cos(q_{shoulder} + q_{elbow}) & l_2 \cdot \cos(q_{shoulder} + q_{elbow}) \end{bmatrix}$$

$\hat{\tau}_{env}$: estimated torque and calculated using $\hat{\tau}_{env} = \sum_i w_i \cdot g_i(\underline{z})$.

Then, we calculate the joint velocity and position for the next time step by integrating this acceleration. The parameters for this simulation were K_p = [15 6; 6 16] kg^2·m^2/s^2, K_v = 0 .15· K_p, l_1= 0.33 m, l_2= 0.34 m, a_1 = 1.5187 kg, a_2 = 0.3442 kg·m, a_3 = 0.0667 kg·m^2, and a_4 = 0.0968 kg·m^2.

Evidence for spatial generalization in the trial-to-trial variability

We hypothesized that the variability in the center movements as shown in Fig. 2a was due to generalization of errors from neighboring movements. For example, after a movement in the right spatial location, rightward forces experienced in that location should generalize to the center movement, causing a leftward after-effect. This point is illustrated for three consecutive movements in Fig. s-1a. The sequence of movements is center-right-center. The error in the first center movement (#301, 49th movement in the set) is small. This movement is followed by a movement at the right, where a large error is experienced (#302). This is followed by another movement at the center (#303), where a large change in the opposite direction is observed. It appears that when two movements at the center have an intervening movement at either the left or right, that intervening movement affects the upcoming movement at the center. In the group with the larger separation distance, no such effect is apparent (Fig. s-1b).

To quantify whether there was a consistent pattern to this interference between movements, we plotted the change of error from one center movement to the next as a function of the number of field trials between them (Fig. s-1c). For example, when the target sequence is center-left-right-left-center, the value on the ordinate is –1 (one right movement minus two left

movements) and the abscissa value is the difference in error between the first and last movements in the sequence. If the force experienced at the left or right influences the expected force at the center, the movements in the center will show increased compensation for rightward force when there are more movements at right and increased compensation for leftward force when there are more movements at left. The magnitude of the change in error measures the influence of side movements on the center movement. We found that this influence, as quantified by the slope of the lines in Fig. s-1c, is larger in the group with the smaller distance. That is, as the neighboring movements became closer, the effect on the center movement became stronger.

In this analysis, we treated sequence C-L-R-C, C-C, and C-R-L-C as if they would affect the second center movement by the same amount ignoring the temporal effect. To eliminate this complex temporal-effect, we also did the same analysis using only sequences C-L-L-C, C-L-C, C-C, C-R-C, and C-R-R-C. However, we do not find any significant difference (equations form linear regression: y = - 0.17x - 0.43, y = - 0.18x - 0.45, y = - 0.086x - 0.21, and y = 0.064x - 0.16 for each group).

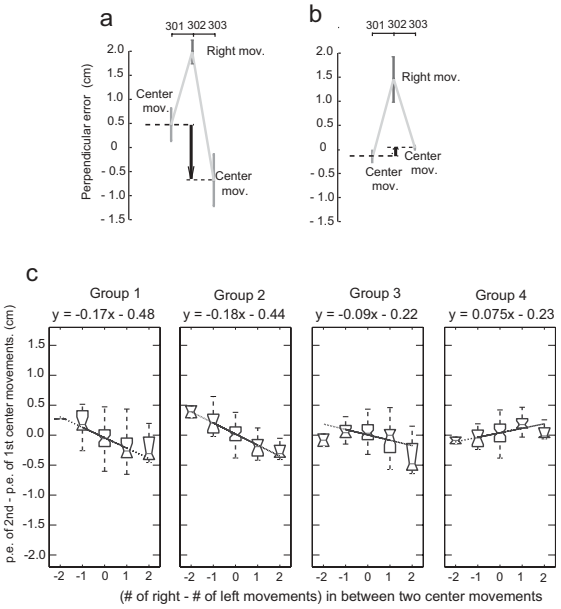

Figure s- 1 Measures of interference. (a) Expanded view of movement errors in movements 301 to 303 in Fig. 2(a). The arrow indicates change of expected force at center after *movement 302* (right movement) in Fig. 2(a). **(b)** Movement errors in movements 301 to 303 in Fig. 2(b). **(c)** Abscissa is the difference between the number of fielded movements on the right and the number of fielded movements on the left between two center movements. Ordinate is change of *p.e.* from the first movement in the center to the second movement in the center. The box has lines at the lower quartile, median, and upper quartile values. The whiskers are lines extending from each end of the box to show the range of the data. The gray line superimposed on each plot is a linear regression, and the equation of the line is shown. A steeper slope indicates a greater influence of the intervening movements.